Biomaterials Science

ROYAL SOCIETY OF CHEMISTRY

MINIREVIEW

View Article Online
View Journal | View Issue

Check for updates

Cite this: *Biomater. Sci.*, 2020, **8**, 2102

Methylcellulose – a versatile printing material that enables biofabrication of tissue equivalents with high shape fidelity

T. Ahlfeld, † V. Guduric,† S. Duin, A. R. Akkineni, K. Schütz, D. Kilian, J. Emmermacher, N. Cubo-Mateo, F. Dani, M. v. Witzleben, J. Spangenberg, R. Abdelgaber, R. F. Richter, A. Lode and M. Gelinsky *

With the aid of biofabrication, cells can be spatially arranged in three dimensions, which offers the opportunity to guide tissue maturation in a better way compared to traditional tissue engineering approaches. A prominent technique allowing biofabrication of tissue equivalents is extrusion-based 3D (bio)printing, also called 3D (bio)plotting or robocasting, which comprises cells embedded in the biomaterial (bioink) during the fabrication process. First bioprinting studies introduced bioinks allowing either good cell viability or good shape fidelity. Concepts enabling printing of cell-laden constructs with high shape fidelity were developed only rarely. Recent studies showed the great potential of the polysaccharide methylcellulose (mc) as supportive biomaterial that can be utilized in various ways to enable biofabrication and especially extrusion-based bioprinting of bioinks. This minireview highlights the multiple applications of mc for biofabrication: it was successfully used as sacrificial ink to enable 3D shaping of cell sheets or biomaterial inks as well as as internal stabilizing component of various bioinks. Moreover, a brief overview about first bioprinted functional tissue equivalents is given, which have been fabricated by using mc. Based on these studies, future research should consider mc as an auxiliary material for bioinks and biofabricated constructs with high shape fidelity.

Received 6th January 2020,
Accepted 25th March 2020

DOI: 10.1039/d0bm00027b

rsc.li/biomaterials-science

Open Access Article. Published on 26 March 2020. Downloaded on 1/19/2026 11:27:28 PM.
This article is licensed under a Creative Commons Attribution-NonCommercial 3.0 Unported Licence.

Introduction

Bioprinting has emerged as a powerful tool for the fabrication of highly hierarchical, organized tissue equivalents, comprising cells, bioactive molecules and biomaterials in a spatially defined arrangement.[1,2] Previously, it has been postulated that bioprinting of cell-laden (hydrogel) matrices, the bioinks,[3] of low polymeric content would be beneficial for the cellular response in bioprinted constructs as the consequential high amount of water is favourable for cell survival, cell migration and diffusion of nutrients, but poor shape fidelity of the fabricated constructs must be expected.[4] The shape fidelity can be defined as the difference of the real printed construct to the related sliced CAD file. For example, poor shape fidelity is a result of fusing of printed features (especially strands fabricated by extrusion-printing), which annihilates the desired inner and outer geometry. Structures fabricated with bioinks of high viscosity resulting from high polymeric content would generate a printed structure of good shape fidelity, since they exhibit a high number of crosslinks, but on the other hand a low cell viability in the bioprinted construct must be expected due to the stiffer and denser hydrogel compromising cellular activities and diffusion processes.[4] However, printing with high shape fidelity is mandatory for most type of tissues, because it allows the fabrication of volumetric and clinically relevant constructs with a controllable spatial distribution of cells. To enable bioprinting of volumetric constructs several approaches have been investigated,[5,6] amongst them visible light-crosslinking,[7] *in situ* UV-crosslinking,[8] multichannel printing with stiff and grid-forming materials[9] and FRESH bioprinting (*e.g.* printing into a gelatin microparticle-based support bath).[10] However, these approaches are limited in the choice of materials and application, due to the high technical efforts which need to be performed, the unclear/potentially harmful effect of photoinitiators on cells[11] or the simple circumstance that stiff (supporting) materials will not be applicable for soft tissues.

As an alternative strategy, many groups investigated blending of hydrogels with additional materials for internal stabilization during fabrication in order to develop novel bioinks, enabling both, enhanced shape fidelity and good cell

Centre for Translational Bone, Joint and Soft Tissue Research, University Hospital Carl Gustav Carus and Faculty of Medicine of Technische Universität Dresden, 01307 Dresden, Germany. E-mail: michael.gelinksy@tu-dresden.de
† These authors contributed equally.

This journal is © The Royal Society of Chemistry 2020

Open Access Article. Published on 26 March 2020. Downloaded on 1/19/2026 11:27:28 PM.
This article is licensed under a Creative Commons Attribution-NonCommercial 3.0 Unported Licence.

response. Deducing results from injectable hydrogels, methylcellulose has been coming up as a promising candidate for bioprinting, either alone or in a blend. The following minireview summarises recent advances in the field of biofabrication of tissue constructs using methylcellulose.

Physicochemical properties of methylcellulose

Methylcellulose (mc) is an ether derivative of cellulose, which is synthesized by substitution of the hydrogen atom from the hydroxy group with a methyl group at the positions C-2 and/or C-3 and/or C-6 (Fig. 1). The properties of mc were extensively reviewed previously,[12,13] therefore the following section summarises just the most important properties of mc for biofabrication.

MC is a non-toxic and biocompatible polymer, which is an administered food and drug additive in Europe, in the USA and most other countries in the world.[14–16] It is hydrophilic in sol state, but the gelation process increases its hydrophobic properties.[17] In contrast to cellulose (as well as nanocellulose and microfibrillar cellulose), mc is soluble in aqueous media. In the cellulose molecule, hydrogen bonds are formed between the hydroxyl groups.[12] These interactions lead to a very ordered, crystalline structure of cellulose which hinders penetration by water molecules. The methoxy groups within the mc disturb the hydrogen bonds allowing water molecules to enter the polysaccharidic structure and to electrostatically bind to the polar side chains. However, since the methyl groups are non-polar, an increasing degree of substitution (DS) finally decreases the solubility of mc in aqueous media.[18,19] Therefore, the usual DS values of mc are below 2.5[12] for tissue engineering purposes, accordingly all studies presented in the following sections dealt with mc with a DS of 1.5–1.9, which is the optimized range for solubility. When the DS is in the range 2.5–3.0, mc can be dissolved in polar organic solvents.[12] Crucial for (bio)printing applications, the high binding affinity of the polar mc to water molecules in aqueous solutions allows the formation of highly viscous hydrogel networks.

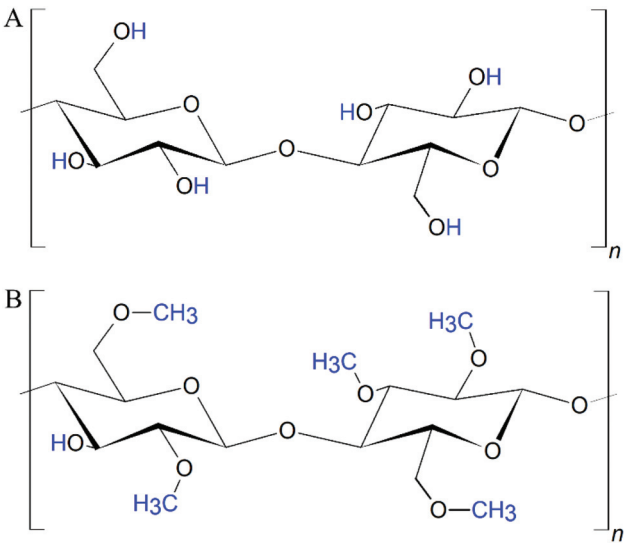

Fig. 1 Structural formula of (A) cellulose and (B) partially substituted methylcellulose. The hydrogen atoms of the respective hydroxy groups are substituted by methyl groups, leading to methoxy (ether) residues.

Generally, mc is a thermo-gelling polymer, which is in sol-state at low temperatures and in gel-state at high temperatures. The gelation process is fully reversible without restrictions. The gelation temperature, as well as the gel strength, are dependent on the DS, concentration and molecular weight (M_w) of mc as well as on electrolyte concentrations.[17,20–24] In brief, an increasing DS and mc concentration will decrease the gelation temperature,[25] whereas increasing M_w will especially enhance the gel strength. Increased ionic strength, caused *e.g.* by salts, dissolved in addition in the aqueous system have the potential to influence gelation temperature and gel strength in both directions.

Crucial for tissue engineering applications is the sterility of mc. Usually the crude mc powder is sterilised before dissolving it in an aqueous solution because the high viscosity of mc-containing solutions impairs the feasibility of methods like sterile-filtration, although it was also reported in literature.[26] Recently, the effect of autoclaving, supercritical CO_2 treatment as well as UV- and γ-irradiation on mechanical and biological properties of mc, blended with alginate, was investigated.[24] γ-Irradiation induced reduction of alginate-mc viscosity and stability, while the other three methods effected only negligible changes of both, shear-thinning behaviour and viscosity. This was caused by a distinct decrease of the molecular mass of mc in the case of γ-irradiation.[24]

Sannino *et al.* discussed the *in vivo* degradability of cellulose and its derivatives extensively, stating that not all reactions have been understood.[13] Nevertheless, the degradation products of mc are glucose molecules, which could act as nutrients for cells. By modification of the functional groups, hydroxypropyl methylcellulose (hpmc) and carboxy methylcellulose (cmc) can get synthesized and have been applied for printing as well.[27,28] In comparison to hpmc and cmc, mc demonstrated the highest enzymatic degradation.[29] However, human cells cannot produce cellulases and degradation can possibly occur only as a consequence of mechanical disruption and due to swelling, macrophage interaction and dissolution.

Influence of molecular weight and gelation of methylcellulose on printability

Next to shear thinning and recovery, a main rheological property of printable inks is their viscosity. A highly viscous ink usually shows a good printability and allows biofabrication with high shape fidelity. The viscosity of mc-based inks is

Open Access Article. Published on 26 March 2020. Downloaded on 1/19/2026 11:27:28 PM.
This article is licensed under a Creative Commons Attribution-NonCommercial 3.0 Unported Licence.

especially dependent on the molecular weight and the gelation point.

The viscosity of a mc solution is directly proportional to the concentration.[30,31] Further, with increasing molecular weight, the viscosity of a 2% solution was shown to increase as well.[30] The biopolymeric character of mc leads to a high polydispersity index ($M_w \cdot M_n^{-1}$),[24] raising problems of unpredictability of the molecular weight, since it contains a high different chain sizes. Due to this reason, commercially available mc usually is characterized by its viscosity (of a 2% solution at 20 °C) and the molecular weight is a recalculated value, which does not allow drawing conclusions for the distribution of the molecular weight. We found that most studies[32–41] used an mc with a given viscosity of 4000 mPa s ($M_n \approx 86$ kDa);[30] these studies have in common to have achieved printing of multiple layers and only limited collapse of predesigned macropores. Other studies[42,43] reported about the use of mc with a given viscosity of 15 mPa s ($M_n \approx 14$ kDa) and found significant improvements of the printed shape fidelity in presence of mc compared to mc-free controls, but those structures lacked the evidence of multiple layer stacking. In a comparative study it could be demonstrated that decreasing the molecular weight of mc evoked a dramatic deterioration on the printability.[24]

Another important criterion for the stability of a mc solution, and thus of a printed structure in pre- and post-crosslinking state, is its gelation. The temperature-dependent gelation point of mc gels decreases with increasing concentration.[21,41,44] In comparison to 6% and 8%, a 10% mc ink with the lowest gelation point demonstrated best printability,[41] indicating that the printability is improved when mc is processed in sol state near the gelation point. The gelation of mc can be influenced by the presence of diluted salts. It could be shown that the gelation temperature can vary strongly (20–60 °C) depending on the concentration and composition of the diluted salts.[21,44] For example, phosphate buffered saline solutions with 2% mc have a gelation temperature of 60 °C, whereas a 100 mM Na_2SO_4 solution with 2% mc leads to gelation at 37 °C.[21] Thus, the stability of printed mc-containing constructs, as well as their degradation behaviour can be controlled by the presence of salts in the (bio-)ink and the cell culture medium. The best printing results of salt-doped mc-inks were achieved by printing in the range of 20–25 °C,[39,40] which created the optimum for viscous behaviour of mc in sol form near to the gelation state.

Methylcellulose as support ink for biofabrication

Since the gelation process of mc is fully reversible and mc is water-soluble in non-gelled state, it can act as support ink for printing (also called sacrificial or fugitive ink). For example, highly viscous mc pastes can be printed and later removed by decreasing the temperature or changing environmental conditions.

That strategy was applied for enhanced cell sheet engineering utilizing the strong dependence of the gelation process of mc on electrolyte concentrations.[21,25] MC solutions of a concentration of 8 wt% were prepared in salt-containing solutions and printed in ring-like structures with high shape fidelity (outer diameter 10 mm, inner diameter 6 mm, the obtained printed structures revealed the same dimensions).[39,40] Afterwards, fibroblasts and endothelial cells were seeded on top; non-printed bulk samples acted as controls. Due to the saline mc solution, mc was in gel state at 37 °C and thus, the printed and cell-seeded structures were stable in cell culture conditions.[21,40] After 20 min incubation at 4 °C, it was possible to remove cell layers by dissolving the mc structures. Interestingly, both cell types responded to the printed ring-like structure and displayed a matching morphology, which was not observed by the cells cultured on the bulk hydrogels.[40]

A similar strategy was investigated for the fabrication of complex scaffold structures.[41] In that work, the printing properties of 6%, 8% and 10% mc sacrificial pastes were investigated and the 10% mc was used as sacrificial ink for 3D extrusion-printing of calcium phosphate cement scaffolds. After setting of the calcium phosphate cement, the mc sacrificial ink was eliminated in a water bath cooled to 4 °C.[41] This allowed the fabrication of real anatomical structures like a scaphoid bone containing a various number of non-printable overhangs and concave/convex surfaces and cavities ($15 \times 15 \times 15$ mm^3 in a $25 \times 25 \times 25$ mm^3 cube) within scaffolds by using extrusion-based printing under mild, cell-compatible conditions.[41]

Additionally, a 3D printed 9%-mc/5%-gelatin blend was used as support structure for a casted cell-laden alginate dialdehyde-gelatin (ADA-GEL) hydrogel.[45] Latest after 7 d of cell culture, the entire support structure was dissolved without disruption of the ADA-GEL structure, which was obtained as open-porous grid or rings with an outer diameter of 5 mm.[45]

Development of novel bioinks including methylcellulose

There are three main bioprinting technologies (laser-assisted, inkjet-based (DOD) and extrusion-based printing) and it was shown that cell-laden mc-bioinks can be processed with all of these methods. An overview about mc-based bioinks, printed cells and the function of mc is shown in Table 1. It was demonstrated that human umbilical vein endothelial cells (HUVEC) can be encapsulated in mc and processed *via* DOD bioprinting.[42] C2C12 mouse myoblast cells were fabricated by extrusion-printing with high cell viabilities using a mc matrix as material component of the bioink.[39] Recently, the LIFT-bioprinting technique was successfully used to produce two different lymphocyte cell lines encapsulated in mc.[46] In case of laser-assisted and DOD bioprinting, the mc matrix acts as a cell carrier, which in the first place enables the spatial deposition of the cells; the finest droplet sizes were in ranges of approx. 100 μm and 90–200 μm for DOD and LIFT, respectively.[42,46] In extrusion-based bioprinting, the mc

 This journal is © The Royal Society of Chemistry 2020

Open Access Article. Published on 26 March 2020. Downloaded on 1/19/2026 11:27:28 PM.
This article is licensed under a Creative Commons Attribution-NonCommercial 3.0 Unported Licence.

Table 1 Cell-containing bioinks based on methylcellulose

Bioprinting technique	Bioink composition	Solvent	Bioprinted cells	Cell viability	Function of mc	Ref.
LIFT	0.3% mc	Cell culture medium	C1R-N1-85 Jurkat cell line	68–84%	Cell carrier	46
DOD	1.2% mc	Cell culture medium	HUVEC	n.r.	Cell carrier	42
EP	8% mc	50 mM Na_2SO_4	C2C12	80%	Permanent matrix shape fidelity	39
EP	3% alginate–9% mc	PBS	hMSC	65%	Viscosity ↑	32
			Rat pancreatic islets	75%	Shape fidelity ↑	55
			Bovine primary chondrocytes	~65%	Pore formation	24
EP	3% alginate–9% mc	HBSS	L929	95%	Viscosity ↑ Shape fidelity ↑	33
EP	3% alginate–9% mc	Water	Algae	80–90%	Viscosity ↑ Shape fidelity ↑	48–50
EP	3% alginate–9% mc	Blood plasma	hTERT-MSC Human osteoblasts Human dental pulp stem cells	80%	Viscosity ↑ Shape fidelity ↑	36
EP	2% alginate–2/4% mc	Water	pMSC	80%	Viscosity ↑ Pore formation	47
EP	3% LAPONITE®–3% alginate–3% mc	Water	hTERT-MSC	75%	Viscosity ↑ Shape fidelity ↑	34
EP	4% alginate–4% halloysite–1% PVDF –3% mc	PBS	Human chondrocyte cell line	n.r.	Viscosity ↑ Shape fidelity ↑	38
EP	2% alginate–2% halloysite–1% RO–2% mc	PBS	Human chondrocytes	n.r.	Viscosity ↑	54
EP	0.9% agarose–2.8% alginate–3% mc	Water	Basil plant cells	n.r.	Viscosity ↑ Shape fidelity ↑	35
EP	8% GelMa–5% mc	50 mM Na_2SO_4	Human osteoblasts	90%	Viscosity ↑ Shape fidelity ↑	52
EP	2% hyaluronic acid–7% mc	PBS	sMSC	85%	Viscosity ↑ Shape fidelity ↑ Stabilization of the blendstabilization of the blend	26 and 43
EP	2.7% RAD16-I–1.5% mc	PBS + 10% sucrose	hMSC, rMSC	55–65%	Viscosity↑	37

LIFT – laser induced forward transfer, DOD – drop-on-demand printing, EP – extrusion printing, PVDF – polyvinylidene fluoride, RO – Russian olive seed powder, C1R-N1-85 – B-lymphocyte cell line, HUVEC – Human umbilical vein endothelial cells, C2C12 – mouse myoblast cell line, L929 – mouse fibroblast cell line, hMSC – human mesenchymal stem cells, pMSC – porcine mesenchymal stem cells, hTERT-MSC – human telomerase reverse transcriptase mesenchymal stem cells, sMSC – sheep mesenchymal stem cells, rMSC – rat mesenchymal stem cells, n.r. – not reported.

additionally acts as the shape-defining component of the printed construct.

Due to its outstanding rheological properties leading to enhanced printability, mc was blended with other matrix forming biopolymers to make them processable by extrusion-printing with good shape fidelity, since it increases viscosity of aqueous solutions, even though it does not support cell attachment.[20] One of the most investigated bioink blends for extrusion-based bioprinting is the combination of alginate and mc. To the best knowledge of the authors, Schütz *et al.* from our lab published the first article about an alginate-mc blend in 2015 (date of online publication).[32] By addition of 9% mc to a 3% alginate sol (in PBS), the viscosity was increased significantly and bioprinting of more than 50 layers with a human mesenchymal stem cell (hMSC)-laden blend was possible, obtaining scaffolds of high shape fidelity with well-preserved macropores. Moreover, mc was not permanently integrated within the blend but vanished during culture due to the fact that the mc was not crosslinked by the Ca^{2+} ions, used for ionic crosslinking of the alginate fraction after printing.[32] In this blend, mc had two functions: it enhanced the viscosity of the alginate sol and thus strongly increased printability; furthermore, it led to the occurrence of micropores within the gelled bioink over time. Later, these findings were confirmed by Li *et al.*, who evaluated the same composition (in HBSS) as beneficial for bioprinting and furthermore increased the interlayer bonding by dripping trisodium citrate on top of the printed layers.[33] Both studies showed, that the blend allowed fabrication of centimetre-scaled constructs with up to 150 layers and minimal strand distances were approx. 1 mm.[32,33] In contrast, a plotted alginate-structure was not stable in *z*-direction. A single strand plotted with a 250 μm needle had a thickness of 500 μm for alginate but 250 μm for the alginate-mc blend.[33] The pore-forming characteristic of alginate-mc (2% and 2/4%, respectively) blends (in water) was used by Gonzalez-Fernandez *et al.* to fabricate bioprinted tissue constructs for enhanced gene delivery.[47] They showed, that the amount of mc significantly influenced the average pore dia-

Open Access Article. Published on 26 March 2020. Downloaded on 1/19/2026 11:27:28 PM.
This article is licensed under a Creative Commons Attribution-NonCommercial 3.0 Unported Licence.

meter after mc leached out from the bioink. The release of mc could be tailored directing the transfection of host or transplanted cells by controlled gene delivery from the bioink. In the same study, in comparison to mc-free alginates, the post-printing cell viability was significantly increased for low concentrations of mc[47] and decreased for high concentrations.[32] At later time points also for higher concentrations of mc no decrease was detected.[32] Apart from bioprinting of mammalian cells, it was previously shown that the blend of alginate and mc forms a bioink which is suitable for *Green Bioprinting* of micro algae.[48–50] The micro algae could be bioprinted alone and in coculture with mammalian cells in alginate-mc.[48] Crucially, the microalgae did not lose their photosynthetic activity after fabrication and thus might be able to provide oxygen needed by the surrounding mammalian cells.[48] Until now, the interactions of alginate and mc macromolecules are not completely understood. However, taking into account that it was reported several times that mc vanishes from the bioprinted structure,[24,32,47] it can be assumed that it is neither forming polymer–polymer interactions with the alginate chains, nor that the mc component behaves like a crosslinked gel. In this blend, alginate and mc chains should form a semi-interpenetrating network. In brief, mc especially provides structural advantages (increase of viscosity and thus printability, formation of micropores) but does not support the biological response of bioprinted cells.

Further modifications of alginate-mc blends led to bioprinted constructs with enhanced biological performance. By addition of 3% of a synthetic nanoclay (LAPONITE®), the total polymer concentration could be reduced to 9% as a result of electrostatic interactions between the LAPONITE® and alginate chains increasing viscosity[34] and probably inducing a higher recovery rate after extrusion as a result of fast self-organization. Further, the cell viability after printing was higher compared to LAPONITE®-free samples. Volumetric cell-laden scaffolds with horizontal macropores could be achieved (not possible in LAPONITE®-free scaffolds[32]), evidencing excellent shape fidelity for bioprinted constructs.[34] Also halloysite, a tubular shaped nanoclay, was blended with alginate (4%), polyvinylidene fluoride (1%) and mc (3%) at a concentration of 4% obtaining bioprinted scaffolds with stable macropores (0.3 mm strand distance) in 8 layers.[38] Although shear-thinning behaviour and viscosity can be modulated by these nanoclays, both studies showed that the biological response (cell viability and drug loading/release capacity) was improved by the nanoclay while mc contributed significantly to the printing quality. Another approach demonstrated that the addition of 0.9% agarose dramatically increased the zero-shear viscosity of a blend of 3% alginate and 3% mc resulting in improved shape fidelity (obtained horizontal macropores did not collapse in scaffolds with 20 layers).[35] In this blend, mc contributed positively by its shear-thinning behaviour, whereas alginate-agarose alone could not be printed. This biopolymer blend was developed for *Green Bioprinting* with plant cell cultures.[35] Bioprinting of plant cells is a promising manufacturing method for secondary metabolite production in industrial pharmaceutical processes.[35] Recently, the biological response of cells to the 3% alginate–9% mc blend could be significantly enhanced by dissolving the two biopolymers in human blood plasma. Whereas the good printability of the blend combination was maintained (printing of centimetre-scaled complexly shaped constructs with more than 50 layers was demonstrated), the proteins of the blood plasma significantly increased the cell viability and allowed spreading of osteoprogenitor cells within the bioink.[36]

Beside alginate, other (bio-)polymers were blended with mc obtaining improved bioinks providing high shape fidelity and good cytocompatibility. Already in 2012, the printability of 2% hyaluronic acid (HA) blended with 7% mc was described as significantly improved compared to a range of other polymers.[26] However, the first investigations of bioprinted, cell-containing constructs of this bioink formulation were performed by Law *et al.* in 2018. They found that the improved shape fidelity of bioprinted HA-mc scaffolds was caused by the presence of mc, but also by convenient gelation properties of this blend, which are caused by the interaction of the two biopolymers.[43] This interaction has not been completely understood yet, however, it was postulated that the HA coils interact with methoxy groups influencing the gelation process of mc,[51] which seems to favour the printability of the blend. Printed structures revealed a calculated accuracy of approx. 85%.[43] Although the highest printing accuracy was determined for a blend with 1%–3% HA-mc, multiple layer stacking was only possible with higher concentrations of mc. MSC derived from sheep could be mixed with the HA-mc bioink and survived the extrusion printing process. In the bioprinted constructs, the cells could spread, adhere and proliferate.[43] An interesting approach was investigated by Cofiño *et al.*, who designed a novel type of bioink mixing a self-assembling peptide (RAD16-I) with mc. With increasing concentration of mc the printed constructs revealed increasing shape fidelity.[37] The final blend enabled differentiation of bioprinted rat MSC to adipose tissue indicated by formation of intracellular lipid droplets after one week of cell cultivation.[37] In a recent study, the printability of photo-crosslinkable GelMA (8%) was significantly improved by addition of mc (5%).[52] The mc contributed to the blend by an increase of viscosity, shear-thinning behaviour and especially shear-recovery whereas the cell viability of human primary osteoblasts was not impacted in comparison to pure GelMA (90%).[52] More than 100 layers of cylindrical and hexagonal shaped constructs could be printed and the authors reported that printed constructs of a height of 2 cm did not collapse, whereas pure GelMA strands fused together.

Bioprinting of tissue equivalents with the aid of methylcellulose-containing bioinks

The development of those cell-containing bioinks led to successful bioprinting of functional tissue equivalents by means

 This journal is © The Royal Society of Chemistry 2020

Open Access Article. Published on 26 March 2020. Downloaded on 1/19/2026 11:27:28 PM.
This article is licensed under a Creative Commons Attribution-NonCommercial 3.0 Unported Licence.

of bioprinting techniques. Table 1 summarises the different mc-based bioinks and lists the function of mc in the bioink blend.

MC-based inks were combined with various materials depending on the target tissue, *e.g.* stiffer materials such as poly-ε-caprolactone (PCL) or calcium phosphate cement (CPC) were used for bone tissue regeneration applications. The MSC-laden blend of 3% alginate and 9% mc could be combined with a plottable CPC in an alternating strand pattern obtaining a biphasic construct suitable for bone and osteochondral tissue engineering.[53] The CPC acts as bone-like mineralized matrix and the novel biphasic constructs revealed a distinct macroporosity enabling nutrient and oxygen supply in volumetric constructs. The cell viability within the bioink was initially affected at the CPC-bioink interface, but recovered latest after 7 d. Interestingly, between 7 and 21 days, the MSC migrated from the soft bioink onto the stiff CPC strands, where they spread and proliferated, offering a novel strategy to distribute cells in mineralized bone constructs (Fig. 2A).[53]

Hodder *et al.* showed that the same blend could be used in combination with bovine primary chondrocytes for bioprinting of constructs for cartilage regeneration evidenced by positive safranin-O staining after 7 days.[24] In addition, cartilage formation could be demonstrated in a blend of mc and alginate, halloysite nanotubes (HNT) and polyvinylidene fluoride (PVDF).[38] This blend maintained appropriate mechanical properties for cartilage tissue engineering, good cell viability and distribution of chondrocytes filling the pore spaces of the scaffolds. Thanks to the addition of mc and HNT, tensile and compressive strengths of printed scaffolds (669–711 kPa and 329–352 kPa respectively) were higher than those consisting of 3% alginate only (tensile strength is 104–116 kPa) and corresponded to the requirements of artificial cartilage.[38] Beside the enhancement of viscosity, the mc in this blend played the role of a sacrificial ink and was washed out during cell cultivation, forming micropores which positively influenced cell adhesion. In a second study, the same group could show that the long-term cell viability of chondrocytes in this blend was increased when the blend was additionally mixed with seed powder of Russian olive.[54] The positive results obtained *in vitro* were confirmed *in vivo* when the scaffolds were implanted in cartilage defects (4 × 1 mm) in the knees of sheep. Six months post implantation the repaired tissue was hyaline cartilage-like with increased collagen type II expression compared to defects filled only with hydrogel (Fig. 2B).[54]

MC was used by Gonzalez-Fernandez and co-workers to form post-printing pores within a printed hydrogel.[47] The amount of mc allowed gaining control of resulting pore size. Peptide-based plasmid DNA could be incorporated into the bioink and was delivered after printing to stem cells *in vitro*, which consequently enabled non-viral transfection of the MSC. The authors found, that the pore-forming character of vanishing mc in the bioink could be used to control the speed and effectiveness of gene delivery. By spatial mc distribution and thus spatial gene delivery in bioprinted constructs, zonal arranged chondrogenesis and osteogenesis was observed *in vivo* in bilayered constructs. As a result, such constructs can act as enhanced osteochondral tissue grafts (Fig. 2C).[47]

Duin *et al.* encapsulated primary pancreatic islets from rats into an alg-mc blend and plotted the bioink into macroporous 3D constructs.[55] The pancreatic islets were homogenously distributed, and revealed a comparable viability to free control islets. Viability increased over time in bioprinted scaffolds. The islets were metabolically active and secretion of insulin could still be detected 7 days after fabrication (Fig. 2D). Remarkably, the bioprinted islets demonstrated an ability to react to stimulation: release of insulin was low when cultivation was done with low glucose concentration (3.3×10^{-3} M) and high in case of high glucose concentration (16.4×10^{-3} M), confirming the functionality of the islets in the bioprinted constructs.[55]

An ink of the same alginate : mc ratio but higher concentration overall (6% alginate and 18% mc) was used for successful fabrication of a volumetric spinal cord model by multichannel 3D bioprinting, involving induced pluripotent stem cell (iPSC)-derived spinal neuronal progenitor cells (sNPC) and mouse iPSC-derived oligodendrocyte progenitor cells (OPC).[56] These cells were printed in precise positions within 3D printed constructs, controlling the direction of axon growth throughout the scaffold. This complex 3D tissue model was fabricated by sequentially printing the mc-based biomaterial ink creating 3 × 3 continuous channels and printing sNPC-laden bioinks into these channels. Cells could survive with axonal extensions present within the entire scaffold and differentiate into functionally mature neurons (Fig. 2E).[56]

Conclusions and future research directions

This mini review highlights the role of methylcellulose as sacrificial ink or cell-laden bioink in various bioprinting approaches, making many matrix-forming biopolymers printable. Depending on its role in the bioink, mc concentration can be easily tailored, for example, 8–10% seems a very convenient concentration acting as a support ink. It is available in large amounts, not expensive and can be printed in the temperature range suitable for cells, from room temperature to 37 °C. On the other hand, fast dilution (within minutes) can be only achieved at rather low temperatures such as 4 °C (similar to Pluronics) which could cause problems for *in vitro* cell cultures. Since mc is a biopolymer, its molecular weight distribution is rather undefined leading to high polydispersity indices and a certain unpredictability of its behaviour. However, mc was shown to enable high shape fidelity bioprinting by improving the shear thinning profiles and viscosities of polymer blends with only a small and, in case of vanishing mc, not permanent increase of the total polymer concentration. Viscosity, directly affecting printability of mc, is highly sensitive to sterilisation techniques. γ-Irradiation induces a distinct decrease of the molecular mass of mc, reducing viscosity and stability, while autoclaving, supercritical CO_2 treat-

Open Access Article. Published on 26 March 2020. Downloaded on 1/19/2026 11:27:28 PM.
This article is licensed under a Creative Commons Attribution-NonCommercial 3.0 Unported Licence.

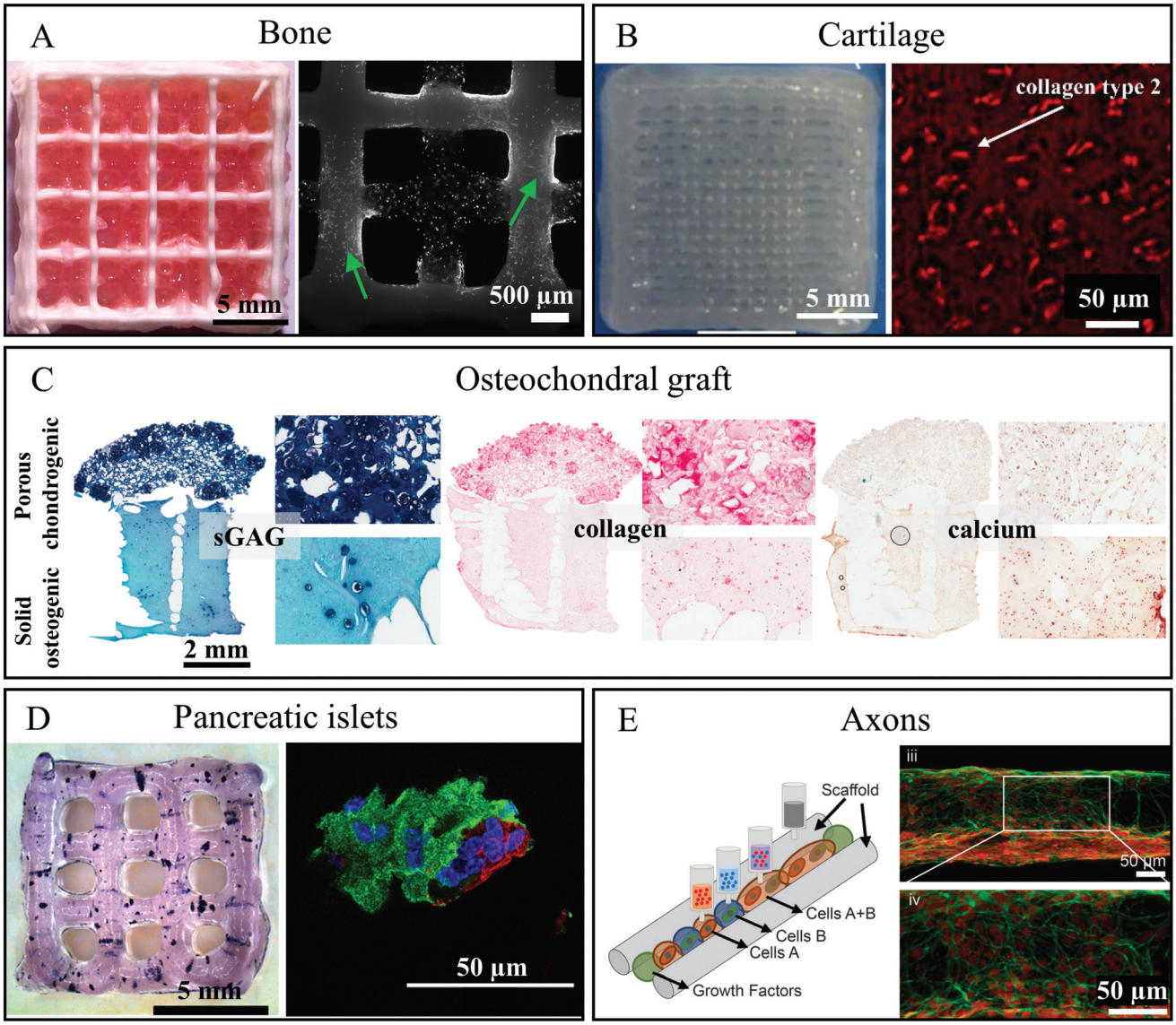

Fig. 2 Functional tissue equivalents which were bioprinted utilising methylcellulose-containing (bio)inks. (A) Left – Photograph of a biphasic CPC/alg-mc scaffold (CPC white, alg-mc red); Right – cLSM image of live/dead stained hTERT-MSC in biphasic scaffolds after 21 days of culture. Green arrows tag adhering and proliferating cell populations on CPC strands. Reproduced from ref. 53 with permission from IOP Publishing, copyright 2019. (B) Left – Photograph of a bioprinted chondrocyte-containing alg-mc/HNT construct; Right – Immunofluorescence staining for expression of collagen type 2 in the constructs containing chondrocytes in articulation defect of sheep after 6 months *in vivo*. Reproduced from ref. 54 with Creative Commons Attribution License, 2019. (C) Histological analysis of sGAG, collagen and calcium in the biphasic graft fabricated using a gene activated bioink after 28 days of culture. Reproduced from ref. 47 with permission from Elsevier, copyright 2019. (D) Left – Bioprinted alg-mc scaffold containing pancreatic islets stained for metabolic activity with MTT 1 day after bioprinting; Right – immunofluorescence stained islet after 7 days cultivation: nuclei (blue), insulin (green) and glucagon (red). Reproduced from ref. 55 with permission from John Wiley and Sons, copyright 2019. (E) Left – Schematic representation of the 3D bioprinting of spinal cord tissue; Right – Image of 3D printed sNPC in a channel after 7 days of culture expressing the mature neuron marker NeuN (red) and the neuron-specific microtubule element β3III-tubulin (green). Reproduced from ref. 56 with permission from John Wiley and Sons, copyright 2019.

ment and UV cause only negligible changes of both, shear-thinning behaviour and viscosity. Solubility of mc in aqueous solutions depends on the tailorable gelation point. Moreover, mc is biologically inert, meaning that neither does it actively contribute to the biological response nor does it interfere with it. The biological function of different tissue equivalents such a bone, axons or that of pancreatic islets was not diminished by mc, but the structural integrity of printed constructs was distinctly improved. Due to the fact that mc is not involved in the crosslinking reaction of the matrix-forming polymers and its inverse thermoreversible gelling mechanism, it is often used to only be a part of the bioink temporarily during fabrication and cleared out afterwards, leaving micropores behind.

 This journal is © The Royal Society of Chemistry 2020

Open Access Article. Published on 26 March 2020. Downloaded on 1/19/2026 11:27:28 PM. This article is licensed under a Creative Commons Attribution-NonCommercial 3.0 Unported Licence.

For these reasons, mc is an intriguing candidate for the development of biofabricated constructs. While the *in vitro* data summarised here are very promising, the field still lacks corresponding *in vivo* data, meaning that an important part of future research in the coming years will likely be oriented in this direction, which will be one step forward in translating mc to clinics.

Author Contribution

TA and VG conceptualised the manuscript, performed the literature research and wrote the major and essential parts of the minireview. SDu, ARA, KS, DK, JE, NCM, FDa, MvW, JS, RA and RFR supported the literature research, discussed the obtained results and assisted to manuscript writing. AL and MG initiated the direction of research, gained funding and wrote and revised the manuscript.

Conflicts of interest

There are no conflicts to declare.

Acknowledgements

The authors thank the German Federal Ministry of Education and Research (BMBF, project InnoPoly, grant number 13XP5067) and the German Research Foundation (DFG, grant number GE 1133/24-1) for financial support. Furthermore, the authors thank the European Social Fund ESF and the Free State of Saxony for the financial support in the course of the ESF Young Researchers Group IndivImp.

Notes and references

1 J. Groll, T. Boland, T. Blunk, J. A. Burdick, D.-W. Cho, P. D. Dalton, B. Derby, G. Forgacs, Q. Li, V. A. Mironov, L. Moroni, M. Nakamura, W. Shu, S. Takeuchi, G. Vozzi, T. B. F. Woodfield, T. Xu, J. J. Yoo and J. Malda, *Biofabrication*, 2016, **8**, 013001.
2 L. Moroni, T. Boland, J. A. Burdick, C. D. Maria, B. Derby, G. Forgacs, J. Groll, Q. Li, J. Malda, V. A. Mironov, C. Mota, M. Nakamura, W. Shu, S. Takeuchi, T. B. F. Woodfield, T. Xu, J. J. Yoo and G. Vozzi, *Trends Biotechnol.*, 2018, **36**, 384–402.
3 J. Groll, J. A. Burdick, D.-W. Cho, B. Derby, M. Gelinsky, S. C. Heilshorn, T. Juengst, J. Malda, V. A. Mironov, K. Nakayama, A. Ovsianikov, W. Sun, S. Takeuchi, J. J. Yoo and T. B. F. Woodfield, *Biofabrication*, 2018, **11**, 013001.
4 J. Malda, J. Visser, F. P. Melchels, T. Jüngst, W. E. Hennink, W. J. A. Dhert, J. Groll and D. W. Hutmacher, *Adv. Mater.*, 2013, **25**, 5011–5028.
5 D. Kilian, T. Ahlfeld, A. R. Akkineni, A. Lode and M. Gelinsky, *MRS Bull.*, 2017, **42**, 585–592.
6 D. Chimene, R. Kaunas and A. K. Gaharwar, *Adv. Mater.*, 2019, 1902026.
7 K. S. Lim, B. S. Schon, N. V. Mekhileri, G. C. J. Brown, C. M. Chia, S. Prabakar, G. J. Hooper and T. B. F. Woodfield, *ACS Biomater. Sci. Eng.*, 2016, **2**, 1752–1762.
8 L. Ouyang, C. B. Highley, W. Sun and J. A. Burdick, *Adv. Mater.*, 2017, **29**, 1604983.
9 W. Schuurman, V. Khristov, M. W. Pot, P. R. van Weeren, W. J. A. Dhert and J. Malda, *Biofabrication*, 2011, **3**, 021001.
10 A. Lee, A. R. Hudson, D. J. Shiwarski, J. W. Tashman, T. J. Hinton, S. Yerneni, J. M. Bliley, P. G. Campbell and A. W. Feinberg, *Science*, 2019, **365**, 482–487.
11 C. Lee, C. D. O'Connell, C. Onofrillo, P. F. M. Choong, C. D. Bella and S. Duchi, *Stem Cells Transl. Med.*, 2020, **9**, 302–315.
12 P. L. Nasatto, F. Pignon, J. L. M. Silveira, M. E. R. Duarte, M. D. Noseda and M. Rinaudo, *Int. J. Polym. Anal. Charact.*, 2015, **7**, 777–803.
13 A. Sannino, C. Demitri and M. Madaghiele, *Materials*, 2009, **2**, 353–373.
14 M. Younes, P. Aggett, F. Aguilar, R. Crebelli, A. D. Domenico, B. Dusemund, M. Filipič, M. J. Frutos, P. Galtier, D. Gott, U. Gundert-Remy, G. G. Kuhnle, C. Lambré, J.-C. Leblanc, I. T. Lillegaard, P. Moldeus, A. Mortensen, A. Oskarsson, I. Stankovic, P. Tobback, I. Waalkens-Berendsen, M. Wright, A. Tard, S. Tasiopoulou and R. A. Woutersen, *EFSA J.*, 2018, **16**, e05047.
15 CFR - Code of Federal Regulations Title 21, https://www.accessdata.fda.gov/scripts/cdrh/cfdocs/cfcfr/CFRSearch.cfm?fr=182.1480, (accessed August 12, 2019).
16 Inactive Ingredient Search for Approved Drug Products, https://www.accessdata.fda.gov/scripts/cder/iig/index.cfm, (accessed July 9, 2018).
17 N. Sarkar, *Carbohydr. Polym.*, 1995, **26**, 195–203.
18 M. Hirrien, J. Desbrières and M. Rinaudo, *Carbohydr. Polym.*, 1996, **31**, 243–252.
19 H. Q. Liu, L. N. Zhang, A. Takaragi and T. Miyamoto, *Cellulose*, 1997, **4**, 321–327.
20 S. Thirumala, J. M. Gimble and R. V. Devireddy, *Cells*, 2013, **2**, 460–475.
21 L. Altomare, A. Cochis, A. Carletta, L. Rimondini and S. Farè, *J. Mater. Sci.: Mater. Med.*, 2016, **27**, 95.
22 P. L. Nasatto, F. Pignon, J. L. M. Silveira, M. E. R. Duarte, M. D. Noseda and M. Rinaudo, *Int. J. Polym. Anal. Charact.*, 2015, **20**, 110–118.
23 N. Sarkar, *J. Appl. Polym. Sci.*, 1979, **24**, 1073–1087.
24 E. Hodder, S. Duin, D. Kilian, T. Ahlfeld, J. Seidel, C. Nachtigall, P. Bush, D. Covill, M. Gelinsky and A. Lode, *J. Mater. Sci. Mater. Med.*, 2019, **30**, 10.
25 N. Contessi, L. Altomare, A. Filipponi and S. Farè, *Mater. Lett.*, 2017, **207**, 157–160.
26 S. V. Murphy, A. Skardal and A. Atala, *J. Biomed. Mater. Res., Part A*, 2013, **101**, 272–284.
27 M. A. Habib and B. Khoda, *Procedia Manuf.*, 2018, **26**, 846–856.

Open Access Article. Published on 26 March 2020. Downloaded on 1/19/2026 11:27:28 PM.
This article is licensed under a Creative Commons Attribution-NonCommercial 3.0 Unported Licence.

28 J. Zhang, W. Yang, A. Q. Vo, X. Feng, X. Ye, D. W. Kim and M. A. Repka, *Carbohydr. Polym.*, 2017, **177**, 49–57.
29 M. G. Wirick, *J. Polym. Sci., Part A-1: Polym. Chem.*, 1968, **6**, 1965–1974.
30 *Methocel Product Sheet*, Dow Chemical, 2013.
31 *Product Information Sheet: Methylcellulose*, Sigma, 1997.
32 K. Schütz, A.-M. Placht, B. Paul, S. Brüggemeier, M. Gelinsky and A. Lode, *J. Tissue Eng. Regener. Med.*, 2017, **11**, 1574–1587.
33 H. Li, Y. J. Tan, K. F. Leong and L. Li, *ACS Appl. Mater. Interfaces*, 2017, **9**, 20086–20097.
34 T. Ahlfeld, G. Cidonio, D. Kilian, S. Duin, A. R. Akkineni, J. I. Dawson, S. Yang, A. Lode, R. O. C. Oreffo and M. Gelinsky, *Biofabrication*, 2017, **9**, 034103.
35 J. Seidel, T. Ahlfeld, M. Adolph, S. Kümmritz, J. Steingroewer, F. Krujatz, T. Bley, M. Gelinsky and A. Lode, *Biofabrication*, 2017, **9**, 045011.
36 T. Ahlfeld, N. Cubo-Mateo, S. Cometta, V. Guduric, C. Vater, A. Bernhardt, A. R. Akkineni, A. Lode and M. Gelinsky, *ACS Appl. Mater. Interfaces*, 2020, **12**, 12557–12572.
37 C. Cofiño, S. Perez-Amodio, C. E. Semino, E. Engel and M. A. Mateos-Timoneda, *Macromol. Mater. Eng.*, 2019, **304**, 1900353.
38 B. Roushangar Zineh, M. R. Shabgard and L. Roshangar, *Mater. Sci. Eng., C*, 2018, **92**, 779–789.
39 N. Contessi Negrini, L. Bonetti, L. Contili and S. Farè, *Bioprinting*, 2018, **10**, e00024.
40 A. Cochis, L. Bonetti, R. Sorrentino, N. Contessi Negrini, F. Grassi, M. Leigheb, L. Rimondini and S. Farè, *Materials*, 2018, **11**, 579.
41 T. Ahlfeld, T. Köhler, C. Czichy, A. Lode and M. Gelinsky, *Gels*, 2018, **4**, 68.
42 L. Gutzweiler, S. Kartmann, K. Troendle, L. Benning, G. Finkenzeller, R. Zengerle, P. Koltay, G. B. Stark and S. Zimmermann, *Biofabrication*, 2017, **9**, 025027.
43 N. Law, B. Doney, H. Glover, Y. Qin, Z. M. Aman, T. B. Sercombe, L. J. Liew, R. J. Dilley and B. J. Doyle, *J. Mech. Behav. Biomed. Mater.*, 2018, **77**, 389–399.
44 H.-F. Liang, M.-H. Hong, R.-M. Ho, C.-K. Chung, Y.-H. Lin, C.-H. Chen and H.-W. Sung, *Biomacromolecules*, 2004, **5**, 1917–1925.
45 D. Dranseikiene, S. Schrüfer, D. W. Schubert, S. Reakasame and A. R. Boccaccini, *J. Mater. Sci. Mater. Med.*, 2020, **31**, 31.
46 A. Márquez, M. G. Fontela, S. Lauzurica, R. Candorcio-Simon, D. M. Martin, M. M. Furio, M. U. Torres, C. T. Morcuende, P. L. Gomez and C. Molpeceres, *Biofabrication*, 2020, **12**, 025019.
47 T. Gonzalez-Fernandez, S. Rathan, C. Hobbs, P. Pitacco, F. E. Freeman, G. M. Cunniffe, N. J. Dunne, H. O. McCarthy, V. Nicolosi, F. J. O'Brien and D. J. Kelly, *J. Controlled Release*, 2019, **301**, 13–27.
48 A. Lode, F. Krujatz, S. Brüggemeier, M. Quade, K. Schütz, S. Knaack, J. Weber, T. Bley and M. Gelinsky, *Eng. Life Sci.*, 2015, **15**, 177–183.
49 F. Krujatz, A. Lode, S. Brüggemeier, K. Schütz, J. Kramer, T. Bley, M. Gelinsky and J. Weber, *Eng. Life Sci.*, 2015, **15**, 678–688.
50 S. Malik, J. Hagopian, S. Mohite, C. Lintong, L. Stoffels, S. Giannakopoulos, R. Beckett, C. Leung, J. Ruiz, M. Cruz and B. Parker, *Glob. Chall.*, 2019, 1900064.
51 L. Mayol, D. De Stefano, F. De Falco, R. Carnuccio, M. C. Maiuri and G. De Rosa, *Carbohydr. Polym.*, 2014, **112**, 480–485.
52 H. Rastin, R. T. Ormsby, G. J. Atkins and D. Losic, *ACS Appl. Bio Mater.*, 2020, **3**, 1815–1826.
53 T. Ahlfeld, F. Doberenz, D. Kilian, C. Vater, P. Korn, G. Lauer, A. Lode and M. Gelinsky, *Biofabrication*, 2018, **10**, 045002.
54 B. Roushangar Zineh, M. R. Shabgard and L. Roshangar, *Adv. Pharm. Bull.*, 2018, **8**, 643–655.
55 S. Duin, K. Schütz, T. Ahlfeld, S. Lehmann, A. Lode, B. Ludwig and M. Gelinsky, *Adv. Healthcare Mater.*, 2019, **8**, 1801631.
56 D. Joung, V. Truong, C. C. Neitzke, S.-Z. Guo, P. J. Walsh, J. R. Monat, F. Meng, S. H. Park, J. R. Dutton, A. M. Parr and M. C. McAlpine, *Adv. Funct. Mater.*, 2018, **28**, 1801850.

 This journal is © The Royal Society of Chemistry 2020